

Fig. 1. Images of the total volume of distribution (V_T) of [^{11}C]SA4503 PET in human brain. Representative images of V_T of [^{11}C]SA4503 PET before and after a single oral administration of donepezil (10 mg) in a healthy subject. Left: image at baseline; right: image after donepezil (10 mg) loading.

donepezil (10 mg) markedly decreased V_T of [^{11}C]SA4503 in the brain (Fig. 1). Figure 2 shows the occupancies of σ_1 receptors in each ROI by donepezil (5 or 10 mg). The mean occupancies by 5 mg and 10 mg donepezil were $58 \pm 11\%$ and $76 \pm 5.3\%$, respectively (Fig. 2).

There were significant correlations between the blood concentration of donepezil and occupancy in all regions (frontal cortex: $\text{ED}_{50} = 5.49$, $r = 0.87$, $p < 0.01$; temporal cortex: $\text{ED}_{50} = 5.40$, $r = 0.80$, $p < 0.05$; parietal cortex: $\text{ED}_{50} = 4.78$, $r = 0.76$, $p < 0.05$; occipital cortex: $\text{ED}_{50} = 5.40$, $r = 0.75$, $p < 0.05$; anterior cingulate gyrus: $\text{ED}_{50} = 5.18$, $r = 0.82$, $p < 0.05$; head of the caudate nucleus: $\text{ED}_{50} = 5.91$, $r = 0.80$, $p < 0.05$; putamen: $\text{ED}_{50} = 7.03$, $r = 0.85$, $p < 0.01$; thalamus: $\text{ED}_{50} = 5.88$, $r = 0.91$, $p < 0.002$; cerebellum: $\text{ED}_{50} = 4.99$, $r = 0.88$, $p < 0.01$) except the hippocampus ($\text{ED}_{50} = 5.05$, $r = -0.09$). Supplementary Fig. S1 (available online) shows representative data of four regions.

Discussion

The major finding of this study is that, after a single oral administration, donepezil bound to σ_1 receptors in the living human brain, in a blood-concentration-dependent manner. To our knowledge, this is the first report demonstrating that donepezil binds to σ_1 receptors in the living human brain at therapeutic doses. This finding is consistent with the previous *in-vitro* receptor-binding data from guinea-pig brain membranes and mouse brain (Kato *et al.* 1999; Kunitachi *et al.* 2009). There are several reports demonstrating a moderate inhibition ($\sim 20\text{--}40\%$) of AChE in the

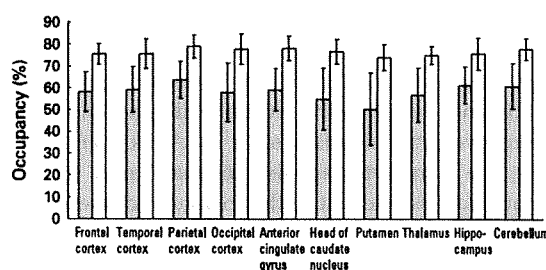


Fig. 2. Occupancies of donepezil of σ_1 receptors in human brain. Presumed occupancies of σ_1 receptors in the brain by 5 mg (\square) and 10 mg (\blacksquare) donepezil were $\sim 60\%$ and $\sim 75\%$, respectively. Figure shows the mean \pm s.d. of four subjects for each dose.

brains of Alzheimer's disease patients after oral administration of donepezil (3, 5 or 10 mg) (Bohnen *et al.* 2005; Kaasinen *et al.* 2002; Shinotoh *et al.* 2001). Taken together, these findings suggest that, at therapeutic doses, donepezil not only inhibits AChE, but also binds to σ_1 receptors in the human brain. Therefore, it is possible that σ_1 receptors are involved in the mechanism of the pharmacological action of donepezil in the human brain.

Maurice *et al.* (2006) reported that dizocilpine-induced learning impairments were attenuated by donepezil, and that this effect was blocked by the σ_1 receptor antagonist BD1047. Furthermore, Meunier *et al.* (2006) reported that donepezil, the σ_1 receptor agonist PRE-084, and the AChE inhibitors (tacrine, rivastigmine, galantamine) showed anti-amnesic effects against intracerebroventricular injection of amyloid β_{25-35} peptide, but only the effects of donepezil and PRE-084 were blocked by BD1047. Very recently, we found that repeated administration of the N-methyl-D-aspartate receptor antagonist phencyclidine significantly decreased the density of σ_1 receptors in the mouse brain (Ishima *et al.* 2009; Kunitachi *et al.* 2009), and that, via σ_1 receptors, donepezil significantly ameliorated phencyclidine-induced cognitive impairments in mice (Kunitachi *et al.* 2009). In addition, we found that donepezil inhibited [^3H](+)-pentazocine (a selective σ_1 receptor ligand) binding with high affinity ($\text{IC}_{50} = 29.12$ nm, Kunitachi *et al.* 2009). These findings suggest that the effect of donepezil is not only based on its AChE inhibition but also its action through σ_1 receptors.

Recently, Hayashi & Su (2007) reported that the endoplasmic reticulum (ER) protein σ_1 receptor, which has also been implicated in neuroprotection and neuroplasticity, is a Ca^{2+} -sensitive and ligand-operated receptor chaperone at the mitochondrion-associated ER

membrane. This suggests that σ_1 receptors play important roles in ER mitochondrial interorganelle Ca^{2+} signalling and in cell survival. Considering the role of ER and mitochondria in the pathophysiology of neuropsychiatric diseases such as Alzheimer's disease, the σ_1 receptor agonist donepezil may exhibit unique actions relevant to the treatment of these diseases.

In conclusion, we demonstrated that donepezil binds to σ_1 receptors in the living human brain at therapeutic doses. Therefore, it is likely that σ_1 receptors may be involved in the mechanism of the pharmacological action of donepezil in the human brain.

Note

Supplementary material accompanies this paper on the Journal's website (<http://journals.cambridge.org/pnp>).

Acknowledgements

This work was supported by a Grant-in-Aid for Scientific Research (no. 19390301 to K.H. and no. 20390334 to K.I.) from the Japan Society for the Promotion of Science. We thank Drs Masaya Hashimoto, Kenji Ishibashi, and Takahiro Saito, Mr Kunpei Hayashi and Ms. Hiroko Tsukinari for technical assistance.

Statement of Interest

None.

References

- Blennow K, de Leon MJ, Zetterberg H (2006). Alzheimer's disease. *Lancet* **368**, 387–403.
- Bohnen NI, Kaufer DI, Hendrickson R, Ivanco LS, et al. (2005). Degree of inhibition of cortical acetylcholinesterase activity and cognitive effects by donepezil treatment in Alzheimer's disease. *Journal of Neurology, Neurosurgery, and Psychiatry* **76**, 315–319.
- Hashimoto K, Ishiwata K (2006). Sigma receptor ligands: possible application as therapeutic drugs and as radiopharmaceuticals. *Current Pharmaceutical Design* **12**, 3857–3876.
- Hayashi T, Su TP (2004). Sigma-1 receptor ligands: potential in the treatment of neuropsychiatric disorders. *CNS Drugs* **18**, 269–284.
- Hayashi T, Su TP (2007). Sigma-1 receptor chaperones at the ER-mitochondrion interface regulate Ca^{2+} signaling and cell survival. *Cell* **131**, 596–610.
- Innis RB, Cunningham VJ, Delforge J, Fujita M, et al. (2007). Consensus nomenclature for in vivo imaging of reversibly binding radioligands. *Journal of Cerebral Blood Flow and Metabolism* **27**, 1533–1539.
- Ishikawa M, Ishiwata K, Ishii K, Kimura Y, et al. (2007). High occupancy of sigma-1 receptors in the human brain after single oral administration of fluvoxamine: a positron emission tomography study using [^{11}C]SA4503. *Biological Psychiatry* **62**, 878–883.
- Ishima T, Fujita Y, Kohno M, Kunitachi S, et al. (2009). Improvement of phencyclidine-induced cognitive deficits in mice by subsequent subchronic administration of fluvoxamine, but not sertraline. *Open Clinical Chemistry Journal* **2**, 7–11.
- Ishima T, Nishimura T, Iyo M, Hashimoto K (2008). Potentiation of nerve growth factor-induced neurite outgrowth in PC12 cells by donepezil: role of sigma-1 receptors and IP3 receptors. *Progress in Neuropsychopharmacology and Biological Psychiatry* **32**, 1656–1659.
- Ishiwata K, Oda K, Sakata M, Kimura Y, et al. (2006). A feasibility study of [^{11}C]SA4503-PET for evaluating sigma receptor occupancy by neuroleptics: the binding of haloperidol to sigma₁ and dopamine D₂-like receptors. *Annals of Nuclear Medicine* **20**, 569–573.
- Kaasinen V, Nagren K, Jarvenpaa T, Roivainen A, et al. (2002). Regional effects of donepezil and rivastigmine on cortical acetylcholinesterase activity in Alzheimer's disease. *Journal of Clinical Psychopharmacology* **22**, 615–620.
- Kato K, Hayako H, Ishihara Y, Marui S, et al. (1999). TAK-147, an acetylcholinesterase inhibitor, increases choline acetyltransferase activity in cultured rat septal cholinergic neurons. *Neuroscience Letters* **260**, 5–8.
- Kawamura K, Ishiwata K, Tajima H, Ishii S, et al. (2000). In vivo evaluation of [^{11}C]SA4503 as a PET ligand for mapping CNS sigma₁ receptors. *Nuclear Medicine and Biology* **27**, 255–261.
- Kimura Y, Naganawa M, Sakata M, Ishikawa M, et al. (2007). Distribution volume as an alternative to the binding potential for sigma₁ receptor imaging. *Annals of Nuclear Medicine* **21**, 533–535.
- Kunitachi S, Fujita Y, Ishima T, Kohno M, et al. (2009). Phencyclidine-induced cognitive deficits in mice are ameliorated by subsequent subchronic administration of donepezil: role of sigma-1 receptors. *Brain Research* **1279**, 189–196.
- Logan J, Fowler JS, Volkow ND, Wang GJ, et al. (1996). Distribution volume ratios without blood sampling from graphical analysis of PET data. *Journal of Cerebral Blood Flow and Metabolism* **16**, 834–840.
- Matsuno K, Nakazawa M, Okamoto K, Kawashima Y, et al. (1996). Binding properties of SA4503 a novel and selective sigma₁ receptor agonist. *European Journal of Pharmacology* **306**, 271–279.
- Maurice T, Meunier J, Feng B, Ieni J, et al. (2006). Interaction with σ_1 protein, but not N-methyl-D-aspartate receptor, is involved in the pharmacological activity of donepezil. *Journal of Pharmacology and Experimental Therapeutics* **317**, 606–614.

- Meunier J, Ieni J, Maurice T** (2006). The anti-amnesic and neuroprotective effects of donepezil against amyloid β_{25-35} peptide-induced toxicity in mice involve an interaction with the σ_1 receptor. *British Journal of Pharmacology* **149**, 998–1012.
- Mintun MA, Raichle ME, Kilbourn MR, Wooten GF, et al.** (1984). A quantitative model for the in vivo assessment of drug binding sites with positron emission tomography. *Annals of Neurology* **15**, 217–227.
- Ohnishi A, Mihara M, Kamakura H, Tomono Y, et al.** (1993). Comparison of the pharmacokinetics of E2020, a new compound for Alzheimer's disease, in healthy young and elderly subjects. *Journal of Clinical Pharmacology* **33**, 1086–1091.
- Sakata M, Kimura Y, Naganawa M, Oda K, et al.** (2007). Mapping of human cerebral sigma₁ receptors using positron emission tomography and [¹¹C]SA4503. *Neuroimage* **35**, 1–8.
- Shinotoh H, Aotsuka A, Fukushi K, Nagatsuka S, et al.** (2001). Effect of donepezil on brain acetylcholinesterase activity in patients with AD measured by PET. *Neurology* **56**, 408–410.

Validation of cardiac ^{123}I -MIBG scintigraphy in patients with Parkinson's disease who were diagnosed with dopamine PET

Kenji Ishibashi · Yuko Saito · Shigeo Murayama ·
Kazutomi Kanemaru · Keiichi Oda · Kiichi Ishiwata ·
Hidehiro Mizusawa · Kenji Ishii

Received: 11 March 2009 / Accepted: 9 June 2009
© Springer-Verlag 2009

Abstract

Purpose The aim of this study was to evaluate the diagnostic potential of cardiac ^{123}I -labelled metaiodobenzylguanidine (^{123}I -MIBG) scintigraphy in idiopathic Parkinson's disease (PD). The diagnosis was confirmed by positron emission tomography (PET) imaging with ^{11}C -labelled 2 β -carbomethoxy-3 β -(4-fluorophenyl)-tropane (^{11}C -CFT) and ^{11}C -raclopride (together designated as dopamine PET).

Methods Cardiac ^{123}I -MIBG scintigraphy and dopamine PET were performed for 39 parkinsonian patients. To estimate the cardiac ^{123}I -MIBG uptake, heart to mediasti-

num (H/M) ratios in early and delayed images were calculated. On the basis of established clinical criteria and our dopamine PET findings, 24 patients were classified into the PD group and 15 into the non-PD (NPD) group.

Results Both early and delayed images showed that the H/M ratios were significantly lower in the PD group than in the NPD group. When the optimal cut-off levels of the H/M ratio were set at 1.95 and 1.60 in the early and delayed images, respectively, by receiver-operating characteristic analysis, the sensitivity of cardiac ^{123}I -MIBG scintigraphy for the diagnosis of PD was 79.2 and 70.8% and the specificity was 93.3 and 93.3% in the early and delayed images, respectively. In the Hoehn and Yahr 1 and 2 PD patients, the sensitivity decreased by 69.2 and 53.8% in the early and delayed images, respectively.

Conclusion In early PD cases, cardiac ^{123}I -MIBG scintigraphy is of limited value in the diagnosis, because of its relatively lower sensitivity. However, because of its high specificity for the overall cases, cardiac ^{123}I -MIBG scintigraphy may assist in the diagnosis of PD in a complementary role with the dopaminergic neuroimaging.

An Editorial Commentary on this paper is available at <http://dx.doi.org/10.1007/s00259-009-1215-9>.

K. Ishibashi · H. Mizusawa
Department of Neurology and Neurological Science,
Graduate School, Tokyo Medical and Dental University,
Tokyo, Japan

K. Ishibashi · K. Oda · K. Ishiwata · K. Ishii (✉)
Positron Medical Center,
Tokyo Metropolitan Institute of Gerontology,
1-1 Nakacho, Itabashi-ku,
Tokyo 173-0022, Japan
e-mail: ishii@pet.tmig.or.jp

Y. Saito
Department of Pathology, Tokyo Metropolitan Geriatric Hospital,
Tokyo, Japan

Y. Saito · S. Murayama
Department of Neuropathology,
Tokyo Metropolitan Institute of Gerontology,
Tokyo, Japan

K. Kanemaru
Department of Neurology, Tokyo Metropolitan Geriatric Hospital,
Tokyo, Japan

Keywords ^{123}I -MIBG · ^{11}C -CFT · ^{11}C -Raclopride ·
Scintigraphy · Positron emission tomography ·
Parkinson's disease

Introduction

Cardiac ^{123}I -labelled metaiodobenzylguanidine (^{123}I -MIBG) scintigraphy has been suggested to be useful for the diagnosis of idiopathic Parkinson's disease (PD), because many recent studies have revealed that cardiac ^{123}I -MIBG uptake decreases with disease progression and that almost all

patients in the advanced stage of PD show decreased cardiac ¹²³I-MIBG uptake [1–5]. However, it is unclear whether cardiac ¹²³I-MIBG uptake is a good surrogate marker for the diagnosis of PD, especially in early and mild PD cases, which are the most difficult to diagnose in daily clinical practice, because the data on the reduction of cardiac ¹²³I-MIBG uptake in the early stage of PD vary greatly among different studies [1–8]. Therefore, we aimed to investigate the sensitivity and specificity of cardiac ¹²³I-MIBG scintigraphy in diagnosing PD, focusing on early and mild cases of PD in the Hoehn and Yahr (HY) stages 1 and 2.

While planning this study, we focused on dividing the patients into PD and non-PD (NPD) groups in the most appropriate manner in order to acquire precise results. Previous studies have shown that the usual clinical diagnostic accuracy of PD ranges from 70 to 90%, and the accuracy rate greatly decreases in early cases [9–12]. In vivo neurofunctional imaging of the basal ganglia, which provides images of both pre- and postsynaptic nigrostriatal dopaminergic functions, has been recognized as a standard marker for the diagnosis of PD in every clinical stage [13–25]. Therefore, in order to improve the accuracy of the diagnosis of PD, especially in early PD cases, and to classify the patients into the PD and NPD groups in a more appropriate manner, we performed positron emission tomography (PET) imaging with ¹¹C-labelled 2β-carbomethoxy-3β-(4-fluorophenyl)-tropane (¹¹C-CFT) and ¹¹C-raclopride. PET imaging with ¹¹C-CFT and ¹¹C-raclopride can assess the levels of presynaptic dopamine transporter (DAT) and postsynaptic dopamine D₂-like receptor (D₂R), respectively, in the striatum. The two types of PET imaging techniques were together designated as dopamine PET. Further, we proposed the definitions of PD and NPD patterns in dopamine PET findings on the

basis of the results which had been confirmed by previous studies.

We also investigated the association between cardiac sympathetic function assessed by cardiac ¹²³I-MIBG uptake, presynaptic nigrostriatal dopaminergic function assessed by striatal ¹¹C-CFT uptake and disease stage determined according to the HY scale.

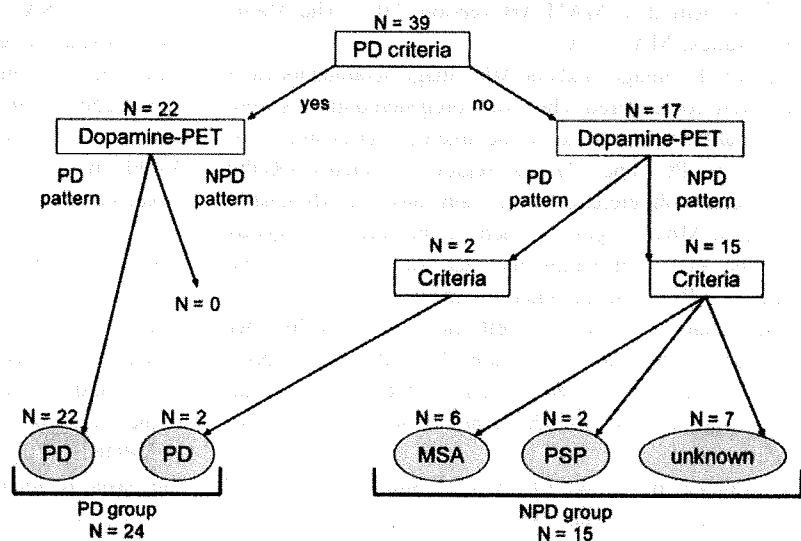
Materials and methods

Subjects

The present study was a retrospective study. The subjects comprised 39 patients who visited the neurological outpatient clinic at Tokyo Metropolitan Geriatric Hospital from November 2001 to October 2007. They chiefly complained of one or more parkinsonian symptoms, including resting tremor, rigidity, bradykinesia and postural instability. The patients were divided into PD and NPD groups (Fig. 1). Cardiac ¹²³I-MIBG scintigraphy, dopamine PET and magnetic resonance imaging (MRI) were performed for all patients. None of the patients had any concomitant hereditary disorder that could cause parkinsonian symptoms. None of the patients had an individual history of any heart disease. Further, none of the patients were on any medication that could cause parkinsonian symptoms.

For dopamine PET, eight healthy subjects (five men and three women) aged 55–74 years [mean±standard deviation (SD) = 62.3±6.9 years] were considered as controls. They were deemed healthy based on their medical history, physical and neurological examinations and MRI of the brain. Further, none of them were on medication.

Fig. 1 Diagnostic flow chart and schematic representation of classification process. Patients were classified into PD and NPD groups on the basis of respective published clinical criteria and our dopamine PET findings



This study protocol was approved by the Ethics Committee of the Tokyo Metropolitan Institute of Gerontology. Written informed consent was obtained from all participants.

PET imaging

PET imaging was performed at the Positron Medical Center, Tokyo Metropolitan Institute of Gerontology by using a SET-2400 W scanner (Shimadzu, Kyoto, Japan) in the three-dimensional scanning mode [26], as described previously [27, 28]. The transmission data were acquired using a rotating $^{68}\text{Ga}/^{68}\text{Ge}$ rod source for attenuation correction. Images of 50 slices were obtained with a resolution of $2 \times 2 \times 3.125$ mm voxels and a 128×128 matrix.

Dopamine PET imaging ^{11}C -CFT and ^{11}C -raclopride were prepared as described previously [29, 30]. The two types of PET imaging were performed for all of the subjects on the same day. The patients being treated with antiparkinsonian drugs underwent dopamine PET following at least 15 h deprivation of the medications. Each subject was administered an intravenous bolus injection of 341 ± 62 (mean \pm SD) MBq of ^{11}C -CFT, followed by that of 311 ± 56 (mean \pm SD) MBq of ^{11}C -raclopride after 2.5–3 h. To measure the uptake of the tracers, static scanning was performed for 75–90 and 40–55 min after the injection of ^{11}C -CFT and ^{11}C -raclopride, respectively. The specific activity of ^{11}C -CFT and ^{11}C -raclopride at the time of injection ranged from 5.9 to 134.2 GBq/ μmol and from 10.2 to 201.7 GBq/ μmol , respectively.

Analysis of dopamine PET images Image manipulations were performed using Dr. View version R2.0 (AJS, Tokyo, Japan) and SPM2 (Functional Imaging Laboratory, London, UK) implemented in MATLAB version 7.0.1 (The MathWorks, Natick, MA, USA).

The two PET images and one MRI image obtained for each subject were coregistered. The three coregistered images were resliced transversally, parallel to the anteroposterior intercommissural (AC-PC) line. Circular regions of interest (ROIs) were selected with reference to the brain atlas and individually coregistered MRI images. In each of the three contiguous slices, one ROI with 8-mm diameter was selected on the caudate, two ROIs on the anterior putamen and two on the posterior putamen on both the left and right sides. In other words, the AC-PC plane and regions 3.1 and 6.2 mm above the AC-PC line were selected. A total of 50 ROIs with 10-mm diameter were selected throughout the cerebellar cortex in five contiguous slices.

To evaluate the uptake of ^{11}C -CFT and ^{11}C -raclopride, we calculated the uptake ratio index by the following

formula [15, 31]: uptake ratio index = (activity in each region – activity in the cerebellum)/(activity in the cerebellum). We previously validated the method to estimate the binding potential of ^{11}C -raclopride and ^{11}C -CFT, adopting the uptake ratio index [27, 28]. For the further analyses, the uptake of each tracer in each subregion of the striatum (the caudate, anterior putamen and posterior putamen) was evaluated as the average value of the left and right sides. The uptake of each tracer in the whole striatum was evaluated as the average value of entire ROIs in the whole striatum.

Cardiac ^{123}I -MIBG scintigraphy

Scintigraphic studies were performed at Tokyo Metropolitan Geriatric Hospital by using a triple-headed gamma camera (PRISM-3000, Shimadzu, Kyoto, Japan). None of the patients were on any medication, i.e. they were not receiving any drugs such as antidepressants and monoamine oxidase inhibitors, which might influence cardiac ^{123}I -MIBG uptake. After a 30-min resting period, each patient was administered an intravenous bolus injection of 111 MBq of ^{123}I -MIBG (Fujifilm RI Pharma Co., Tokyo, Japan). Planar images of the chest in the anterior view were obtained twice for 5 min, starting at 20 min (early phase) and then at 180 min (delayed phase) after the injection of ^{123}I -MIBG. Relative organ uptake of ^{123}I -MIBG was determined by selecting the ROIs on the heart and mediastinum in the anterior planar image [32]. Average counts per pixel in the heart and mediastinum were used to calculate the heart to mediastinum (H/M) ratio.

MRI

MRI was performed at Tokyo Metropolitan Geriatric Hospital. By using a 1.5-T Signa EXCITE HD scanner (GE, Milwaukee, WI, USA), transaxial T1-weighted images [three-dimensional spoiled gradient-recalled (3D SPGR), repetition time (TR) = 9.2 ms, echo time (TE) = 2.0 ms, matrix size = $256 \times 256 \times 124$, voxel size = $0.94 \times 0.94 \times 1.3$ mm] and transaxial T2-weighted images (first spin echo, TR = 3,000 ms, TE = 100 ms, matrix size = $256 \times 256 \times 20$, voxel size = $0.7 \times 0.7 \times 6.5$ mm) were obtained.

Clinical diagnosis

The diagnostic flow chart is shown in Fig. 1. First, the patients were divided into two groups (22 patients in one group and 17 patients in the other) on the basis of the clinical criteria of the UK Parkinson's Disease Brain Bank (UKPDBB) [10]. Each group was then further classified on the basis of dopamine PET findings. As shown in Fig. 2, the PD pattern in dopamine PET was defined as follows: (1)

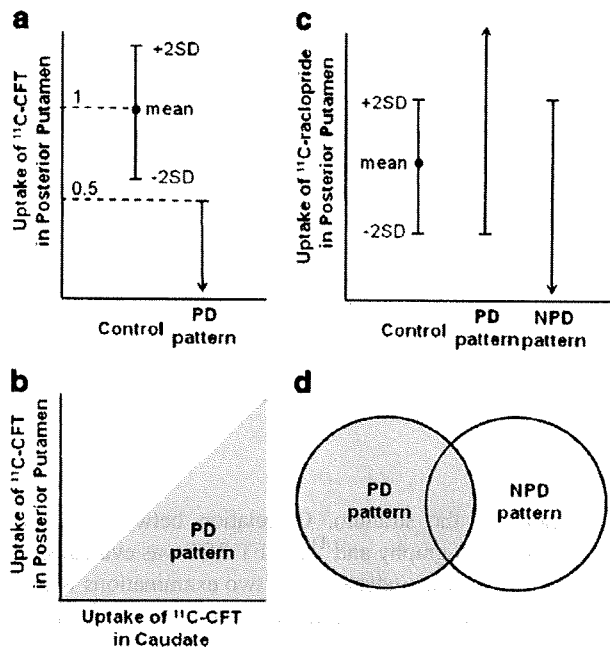


Fig. 2 PD and NPD patterns defined on the basis of dopamine PET findings. PD pattern: ^{11}C -CFT uptake in the posterior putamen of patients less than 50% of the mean uptake in the posterior putamen of normal controls (a) and less than that in the caudate of patients (b); ^{11}C -raclopride uptake in the posterior putamen of patients more than the mean - 2 SD of the uptake in the posterior putamen of normal controls (c). NPD pattern: ^{11}C -raclopride uptake in the posterior putamen of patients less than the mean + 2 SD of the uptake in the posterior putamen of normal controls (c). The patient was considered to be PD pattern when both PD and NPD were fulfilled (d). The uptake in each subregion of the striatum was evaluated as the average value of both sides

^{11}C -CFT uptake in the posterior putamen of the patients less than 50% of the mean uptake in the posterior putamen of normal controls (Fig. 2a) and less than that in the caudate of the patients (Fig. 2b) and (2) ^{11}C -raclopride uptake in the posterior putamen of the patients more than the mean - 2 SD of the uptake in the posterior putamen of normal controls (Fig. 2c). The NPD pattern was defined as follows: ^{11}C -raclopride uptake in the posterior putamen of the patients less than the mean + 2 SD of the uptake in the posterior putamen of normal controls (Fig. 2c). The patient was considered to be PD pattern when both PD and NPD were fulfilled (Fig. 2d).

Statistical analysis

Differences in the averages and variances were tested by Student's *t* test and one-way analysis of variance, respectively. Correlations between the two groups of patients were assessed by linear regression analysis with Pearson's correlation test; *p* values of <0.05 were considered statistically significant.

Results

Patients

Classification into PD and NPD groups All 22 patients who fulfilled the UKPDBB PD criteria at initial diagnosis [10] showed the PD pattern on dopamine PET (Fig. 1). They were classified into the PD group. The other 17 patients were further classified according to dopamine PET findings and respective published clinical criteria. Of the 17 patients, 2 showed the PD pattern on dopamine PET. In fact, the symptom manifested was only resting tremor at initial diagnosis; however, during the course of the study, they fulfilled the UKPDBB PD criteria [10] and were classified into the PD group.

Of the 17 patients, 15 showed the NPD pattern on dopamine PET and were classified into the NPD group (Fig. 1). These patients were then further divided into three subgroups. Six patients fulfilled the multiple system atrophy (MSA) criteria [33]. Two patients fulfilled the progressive supranuclear palsy (PSP) criteria [34]. For the remaining seven patients, no definitive diagnoses could be established despite follow-up for more than 1 year.

Finally, 24 patients (7 men and 17 women, age range: 60–85 years, mean age \pm SD = 71.5 ± 6.8 years) and 15 patients (8 men and 7 women, age range: 65–86 years, mean age \pm SD: 76.0 ± 5.5 years) were classified into the PD and NPD groups, respectively.

Demographic data Patient characteristics are summarized in Table 1. In the PD group, 11 patients were drug naive, 7 were being treated with L-dopa and 6 were being treated with L-dopa and dopamine agonists at the time of dopamine PET. The interval between cardiac ^{123}I -MIBG scintigraphy and dopamine PET was within 6 months for 16 patients, between 6 and 12 months for 1 patient and more than 1 year for 7 patients. However, the HY stage of each patient in the PD group remained the same between cardiac ^{123}I -MIBG scintigraphy and dopamine PET. In the NPD group, 11 patients were not administered any antiparkinsonian drug, and 4 were being treated with only L-dopa. The interval between the two examinations was within 6 months for 12 patients, between 6 and 12 months for 1 patient and more than 1 year for 2 patients.

Uptake of ^{123}I -MIBG

Both the early and delayed images showed significantly lower H/M ratios in the PD group than in the NPD group (Fig. 3). In both the early and delayed images, the H/M ratios tended to decrease with the progression of the HY stages; however, the decrease was not statistically significant.

Table 1 Clinical features of patients in Parkinson's disease and non-Parkinson's disease groups

Groups	Patients		Age (years)	Duration (years)	¹²³ I-MIBG scintigraphy		¹¹ C-CFT PET Uptake ratio index in the whole striatum
	Number	M:F			Heart to mediastinum ratio		
					Early	Delayed	
Parkinson's disease	24	7:17	71.5±6.8	3.5±3.2	1.66±0.45	1.46±0.41	0.98±0.34
Hoehn and Yahr 1	4	0:4	65.0±7.7	2.9±2.6	1.75±0.33	1.49±0.29	1.49±0.40
Hoehn and Yahr 2	9	2:7	73.9±5.6	2.4±1.0	1.81±0.54	1.60±0.45	1.00±0.20
Hoehn and Yahr 3	8	5:3	71.9±7.2	3.0±1.8	1.57±0.44	1.41±0.44	0.81±0.20
Hoehn and Yahr 4	3	0:3	72.3±5.0	9.0±6.1	1.36±0.05	1.12±0.08	0.69±0.07
Non-Parkinson's disease	15	8:7	76.0±5.5	2.8±1.9	2.35±0.46	2.18±0.51	1.65±0.68

Data are expressed as mean±SD

Table 2 shows the sensitivity and specificity of cardiac ¹²³I-MIBG scintigraphy in differentiating patients with PD from the other patients with chief complaints of parkinsonian symptoms. When the optimal cut-off levels of ¹²³I-MIBG were set at 1.95 and 1.60 by receiver-operating characteristic analysis, the sensitivity of cardiac ¹²³I-MIBG scintigraphy for the diagnosis of PD was 79.2 and 70.8% and the specificity was 93.3 and 93.3% in the early image and delayed images, respectively. In HY 1 and 2 PD patients the sensitivity was 69.2 and 53.9% and in HY 3 and 4 PD patients the sensitivity was 90.9 and 90.9% in the early image and delayed images, respectively

Uptake of ¹¹C-CFT

The uptake of ¹¹C-CFT in the whole striatum decreased with the progression of the HY stages (Fig. 4). Significant reduction in the ¹¹C-CFT uptake with the progression of the HY stages was also observed in each of the three

subregions of the striatum. Correlation between cardiac ¹²³I-MIBG scintigraphy and ¹¹C-CFT PET was evaluated in the 16 patients who underwent the two examinations within 6 months. There was no significant correlation between the ¹¹C-CFT uptake in the whole striatum and the H/M ratios in both the early images ($r=0.15, p=0.59$) and delayed images ($r=0.21, p=0.43$) (Fig. 5). Further, no significant correlation was observed between the ¹¹C-CFT uptake in each of the three subregions of the striatum and the H/M ratio.

Discussion

In the present study, we investigated the sensitivity and specificity of cardiac ¹²³I-MIBG scintigraphy in diagnosing PD and differentiating the patients with PD from the others with chief complaints of parkinsonian symptoms. Further, we investigated the correlation between cardiac sympathetic function assessed by cardiac ¹²³I-MIBG uptake, nigrostriatal

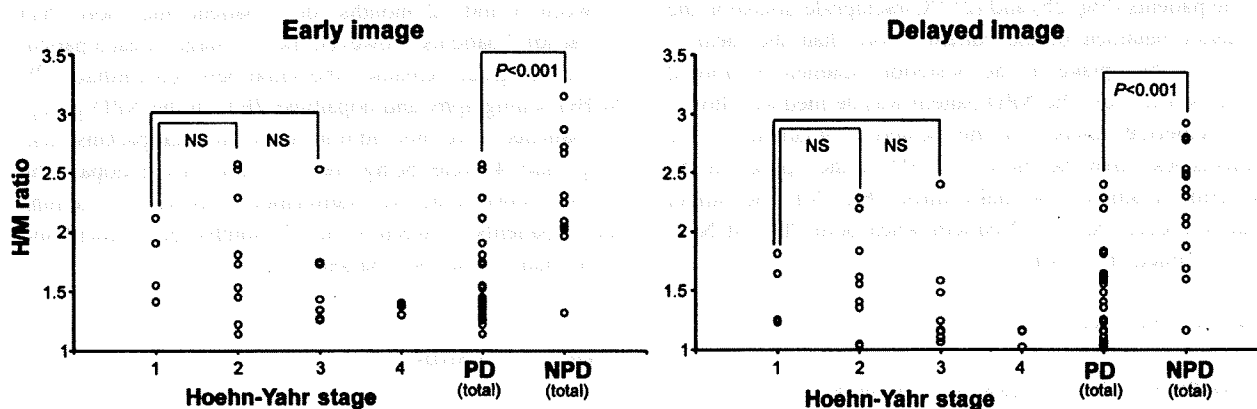


Fig. 3 H/M ratios in the PD and NPD groups in early and delayed images. Each graph represents the relation between the H/M ratio and Hoehn and Yahr stage of PD and a comparison of the H/M ratios of the total number of PD and NPD patients. Both images showed that

the H/M ratios were significantly lower in the PD group than in the NPD group; however, the H/M ratios of patients in HY 1 of PD were not significantly higher than those of the patients in HY 2 and 3 of PD. *NS* not significant

Table 2 Sensitivity and specificity of cardiac ¹²³I-MIBG scintigraphy in differentiating Parkinson's disease from other parkinsonian syndromes

Total PD patients (n=24)												
	Early image						Delayed image					
Cut-off	1.80	1.85	1.90	1.95	2.00	2.05	1.60	1.65	1.70	1.75	1.80	1.85
Sensitivity	70.8%	75.0%	75.0%	79.2%	79.2%	79.2%	70.8%	75.0%	79.2%	79.2%	79.2%	87.5%
Specificity	93.3%	93.3%	93.3%	93.3%	86.7%	80.0%	93.3%	80.0%	73.3%	73.3%	73.3%	73.3%
Hoehn and Yahr 1 and 2 (n=15)												
	Early image						Delayed image					
Cut-off	1.80	1.85	1.90	1.95	2.00	2.05	1.60	1.65	1.70	1.75	1.80	1.85
Sensitivity	53.8%	61.5%	61.5%	69.2%	69.2%	69.2%	53.8%	61.5%	69.2%	69.2%	69.2%	84.6%

Cut-off levels, for which both the sensitivity and specificity were more than 70%, are shown. The optimal cut-off levels determined by receiver-operating characteristic analysis were at 1.95 and 1.60 in the early and delayed images, respectively

dopaminergic function assessed by ¹¹C-CFT uptake and disease stage determined according to the HY scale.

It has been reported that cardiac ¹²³I-MIBG uptake in patients with PD is significantly lower than that in patients with other parkinsonian syndromes [1–7]; this result corresponds to our results. Several reports suggest that the severity of motor impairment and disease duration are correlated with reduced ¹²³I-MIBG uptake in patients with PD [1, 2, 5, 6]; however, some other findings deny such correlations, similar to ours [3, 4, 7, 8]. This discrepancy is presumably explained by the fact that the degree of cardiac ¹²³I-MIBG uptake in patients in HY 1 and 2 of PD varies greatly among different studies. Difficult definitive diagnosis of PD in early and mild cases may also be because of the great variation. On the other hand, almost all patients in the advanced stage of PD have shown very low ¹²³I-MIBG uptake in both the previous and the present studies. Li et al. reported that cardiac sympathetic denervation progresses over time and that the rate of decrease in the number of sympathetic terminals appears to be at least as high as that of nigrostriatal dopaminergic terminals [35]. Therefore, we considered that although the onset of cardiac sympathetic

denervation varied among the patients with PD, severe cardiac sympathetic denervation occurred in all of the patients by the terminal stage of PD. In regard to the association with a sympathetic symptom, it was reported that reduced ¹²³I-MIBG uptake does not always mean the existence of a sympathetic symptom [1, 3, 4, 7]. Also in this study, of the three patients in stage 4 of the HY scale who showed very low ¹²³I-MIBG uptake (Fig. 3), two had orthostatic hypotension; however, the remaining one patient had no cardiovascular sympathetic symptom and showed no abnormality in the head-up tilt test. In contrast to ¹²³I-MIBG uptake, the decrease in ¹¹C-CFT uptake in the whole striatum and in each of its three subregions significantly correlated with disease progression represented by the HY stages, as reported previously [14, 16, 22]. Considering the causal pathophysiological mechanism of PD, this is reasonable because ¹¹C-CFT uptake directly indicates nigrostriatal dopaminergic function.

We investigated the sensitivity and specificity of cardiac ¹²³I-MIBG scintigraphy in diagnosing PD and differentiating the patients with PD from the other patients with chief complaints of parkinsonian symptoms. Similar to the

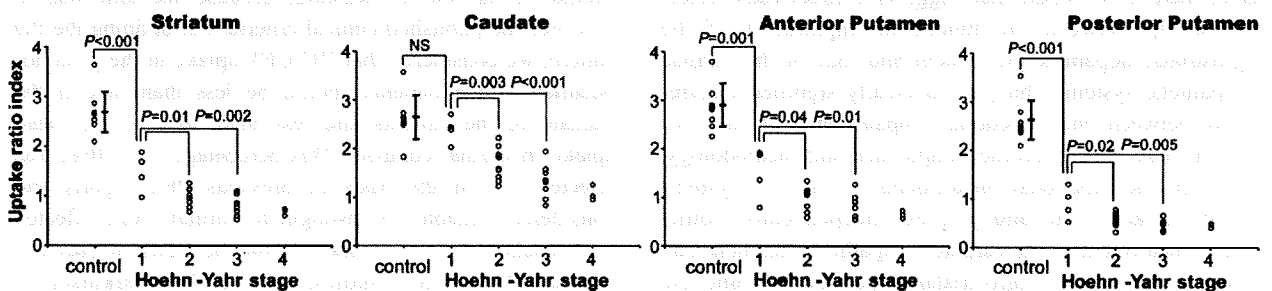


Fig. 4 Relation between the HY stage and uptake ratio index of ¹¹C-CFT in the whole striatum, caudate, anterior putamen and posterior putamen of patients with PD. In all four graphs, the uptakes in the patients in HY 1 of PD are significantly higher than those in the patients in HY 2 and 3 of PD. The uptakes in the caudate of patients in

HY 1 of PD are not significantly higher than those in the caudate of controls, while the uptakes in the whole striatum, anterior putamen and posterior putamen of patients in HY 1 of PD are significantly higher than those in the corresponding regions of the controls. The vertical bar represents the mean ± SD of controls. NS not significant

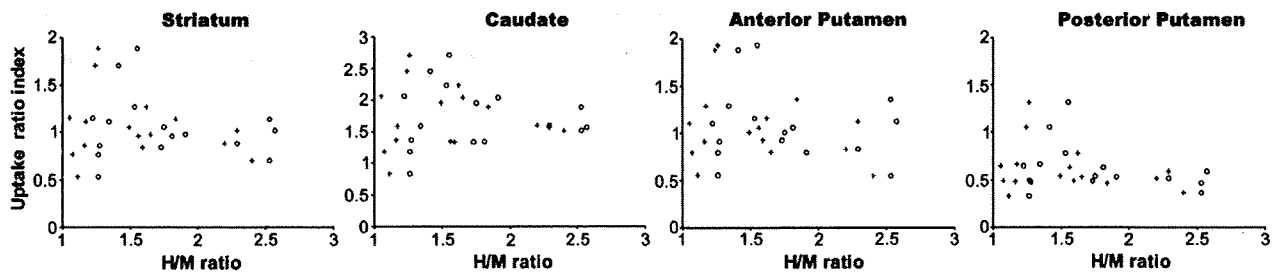


Fig. 5 Relation between the H/M ratio and uptake ratio index of ^{11}C -CFT in the whole striatum, caudate, anterior putamen and posterior putamen of patients with PD. Correlation was evaluated for 16 patients who underwent the two examinations (scintigraphy and PET)

within 6 months. In all four graphs, no significant correlations are observed between the early images (open circles) and delayed images (plus signs)

previous meta-analysis of studies with a total of 246 PD cases [36], in both early and delayed images our study showed high specificity for the overall cases and high sensitivity for the advanced cases. However, early cases tended to have relatively lower sensitivity in both images, although the sample size and methodology greatly differed among the studies. Thus, our results suggested that even in the case of sustained cardiac ^{123}I -MIBG uptake, the possibility of PD should not be denied and follow-up clinical examinations, including ^{123}I -MIBG scintigraphy, should be conducted, especially in early and mild PD cases.

No definite correlation was found either between cardiac ^{123}I -MIBG uptake and striatal ^{11}C -CFT uptake or between cardiac ^{123}I -MIBG uptake and subregional ^{11}C -CFT uptake in the PD group. Two groups have reported the association between the functional impairment of the nigrostriatal dopaminergic system and that of the cardiac sympathetic system [8, 37]. Spiegel et al. ($n=18$) found a correlation between the two indices, i.e. ^{123}I -MIBG and ^{11}C -CFT uptake, while Raffel et al. ($n=9$) found no correlation between them. This discrepancy may be explained as follows. The functional impairment of both the nigrostriatal dopaminergic and cardiac sympathetic systems increases with disease progression, as described earlier; hence, a correlation was observed in some studies. On the other hand, there is no report that suggests a direct cause-effect relationship between the functional impairment of the nigrostriatal dopaminergic system and that of the cardiac sympathetic system. Thus, a statistically significant correlation between the functional impairments of the two systems may depend on the sample size and methodology. However, the functional impairments of the two systems would, in fact, occur and progress independently. Sometimes, impairment of the cardiac sympathetic function may precede that of the nigrostriatal dopaminergic function, while at other times, the latter may precede the former.

This is the first report wherein PD and NPD patterns in dopamine PET findings were defined on the basis of the results which have been confirmed as follows. In presynaptic

DAT images, three characteristic changes are observed [14–16, 22]. First, the reduction in the ^{11}C -CFT uptake in the striatum begins from the posterior putamen, representing the initial locus of PD [38]. Second, the uptake ratio of the posterior putamen to the caudate is less than 1. Third, one putamen is usually more affected than the other, reflecting asymmetric degeneration. In fact, Fig. 4 shows that the ^{11}C -CFT uptake in the posterior putamen markedly decreased in the early stage of PD, while that in the caudate was relatively constant in the early stage. In postsynaptic D_2R images, putaminal uptake is normal or mildly upregulated in untreated PD, presumably as a compensatory response to decrease in presynaptic dopamine [17–19]. On the other hand, in treated or longstanding PD, the uptake restores to the normal level in the putamen and most often decreases in the caudate; this is presumably as a result of long-term downregulation due to chronic dopaminergic therapy or structural adaptation of the postsynaptic dopaminergic system to the progressive degeneration of nigrostriatal neurons [17, 19, 21]. In fact, *in vitro* studies have reported that the densities of striatal D_2Rs are maintained even in the advanced stage [39, 40].

On the basis of the earlier mentioned characteristic changes, especially in the posterior putamen, we defined the PD and NPD patterns such that false-negative cases should be as few as possible, because the aim was to reinforce the published clinical criteria. For defining the PD pattern, we considered that ^{11}C -CFT uptake in the posterior putamen of the patients should be less than that in the caudate of the patients and less than 50% of the mean uptake in normal controls. This percentage (i.e. 50%) was selected (1) on the basis of previous PET reports and considered suitable to distinguish normal from affected individuals [14–16, 22] and (2) on the basis of previous reports of *in vitro* studies, stating that parkinsonian symptoms appear when 80% of the striatal dopamine is lost or 50% of the nigral cells degenerate [38, 41]. Asymmetric uptake was not defined because of the difficulty in determining the intraindividual differences in

the uptake on the left and right sides. However, all 24 patients with PD showed asymmetric uptake. In the ^{11}C -raclopride PET image, since the uptake in the putamen was not less than the normal range, we considered that the uptake in the posterior putamen was normal or increased. For defining the NPD pattern, presynaptic function was not determined because the degree of the presynaptic dysfunction varies with diseases. In the ^{11}C -raclopride PET image, we considered that the uptake in the posterior putamen was normal or decreased because the uptake was not more than the normal range, except for Lewy body disease.

Conclusions

In early and mild PD cases, cardiac ^{123}I -MIBG scintigraphy is of limited value in the diagnosis of PD, because the sensitivity was indicated to be less than 70%. However, because of its high specificity for the overall cases and high sensitivity for the advanced cases, cardiac ^{123}I -MIBG scintigraphy may assist in the diagnosis of PD in a complementary role with the dopaminergic neuroimaging. Disease progression indicated by the HY stages has a stronger association with the nigrostriatal dopaminergic function assessed by striatal ^{11}C -CFT uptake than with the cardiac sympathetic function assessed by cardiac ^{123}I -MIBG uptake. The impairment of the two functions would occur and progress independently.

Acknowledgments The authors thank Mr. Keiichi Kawasaki, Dr. Masaya Hashimoto, and Ms. Hiroko Tsukinari for their technical assistance and useful discussions. This work was supported by grant-in-aid for Scientific Research (B) No. 20390334 (K.I.) from the Japan Society for the Promotion of Science and a grant (06-46) (K.I.) from the Program for Promotion of Fundamental Studies in Health Sciences of the National Institute of Biomedical Innovation of Japan, and a grant-in-aid for Neurological and Psychiatric Research (S.M., Y.S., and Ke.I.), and Research for Longevity (S.M., Y.S., and Ke.I.) from the Ministry of Health, Labor, and Welfare of Japan, a grant-in-aid for Long-Term Comprehensive Research on Age-associated Dementia from the Tokyo Metropolitan Institute of Gerontology (K.K., S.M., and Ke.I.).

References

- Orimo S, Ozawa E, Nakade S, Sugimoto T, Mizusawa H. (123I)-metaiodobenzylguanidine myocardial scintigraphy in Parkinson's disease. *J Neurol Neurosurg Psychiatry* 1999;67:189–94.
- Satoh A, Serita T, Seto M, Tomita I, Satoh H, Iwanaga K, et al. Loss of 123I-MIBG uptake by the heart in Parkinson's disease: assessment of cardiac sympathetic denervation and diagnostic value. *J Nucl Med* 1999;40:371–5.
- Taki J, Nakajima K, Hwang EH, Matsunari I, Komai K, Yoshita M, et al. Peripheral sympathetic dysfunction in patients with Parkinson's disease without autonomic failure is heart selective and disease specific. *taki@med.kanazawa-u.ac.jp. Eur J Nucl Med* 2000;27:566–73.
- Takatsu H, Nishida H, Matsuo H, Watanabe S, Nagashima K, Wada H, et al. Cardiac sympathetic denervation from the early stage of Parkinson's disease: clinical and experimental studies with radiolabeled MIBG. *J Nucl Med* 2000;41:71–7.
- Nagayama H, Hamamoto M, Ueda M, Nagashima J, Katayama Y. Reliability of MIBG myocardial scintigraphy in the diagnosis of Parkinson's disease. *J Neurol Neurosurg Psychiatry* 2005;76:249–51.
- Hamada K, Hirayama M, Watanabe H, Kobayashi R, Ito H, Ieda T, et al. Onset age and severity of motor impairment are associated with reduction of myocardial 123I-MIBG uptake in Parkinson's disease. *J Neurol Neurosurg Psychiatry* 2003;74:423–6.
- Braune S, Reinhardt M, Schnitzer R, Riedel A, Lucking CH. Cardiac uptake of [123I]MIBG separates Parkinson's disease from multiple system atrophy. *Neurology* 1999;53:1020–5.
- Raffel DM, Koeppe RA, Little R, Wang CN, Liu S, Junck L, et al. PET measurement of cardiac and nigrostriatal denervation in Parkinsonian syndromes. *J Nucl Med* 2006;47:1769–77.
- Rajput AH, Rozdilsky B, Rajput A. Accuracy of clinical diagnosis in parkinsonism—a prospective study. *Can J Neurol Sci* 1991;18:275–8.
- Hughes AJ, Daniel SE, Kilford L, Lees AJ. Accuracy of clinical diagnosis of idiopathic Parkinson's disease: a clinico-pathological study of 100 cases. *J Neurol Neurosurg Psychiatry* 1992;55:181–4.
- Jankovic J, Rajput AH, McDermott MP, Perl DP. The evolution of diagnosis in early Parkinson disease. *Parkinson Study Group. Arch Neurol* 2000;57:369–72.
- Hughes AJ, Daniel SE, Lees AJ. Improved accuracy of clinical diagnosis of Lewy body Parkinson's disease. *Neurology* 2001;57:1497–9.
- Plotkin M, Amthauer H, Klaffke S, Kuhn A, Ludemann L, Arnold G, et al. Combined 123I-FP-CIT and 123I-IBZM SPECT for the diagnosis of parkinsonian syndromes: study on 72 patients. *J Neural Transm* 2005;112:677–92.
- Nurmi E, Bergman J, Eskola O, Solin O, Vahlberg T, Sonninen P, et al. Progression of dopaminergic hypofunction in striatal subregions in Parkinson's disease using [18F]CFT PET. *Synapse* 2003;48:109–15.
- Frost JJ, Rosier AJ, Reich SG, Smith JS, Ehlers MD, Snyder SH, et al. Positron emission tomographic imaging of the dopamine transporter with ^{11}C -WIN 35,428 reveals marked declines in mild Parkinson's disease. *Ann Neurol* 1993;34:423–31.
- Rinne JO, Ruottinen H, Bergman J, Haaparanta M, Sonninen P, Solin O. Usefulness of a dopamine transporter PET ligand [(18F)beta-CFT] in assessing disability in Parkinson's disease. *J Neurol Neurosurg Psychiatry* 1999;67:737–41.
- Antonini A, Schwarz J, Oertel WH, Beer HF, Madeja UD, Leenders KL. [^{11}C]raclopride and positron emission tomography in previously untreated patients with Parkinson's disease: influence of L-dopa and lisuride therapy on striatal dopamine D2-receptors. *Neurology* 1994;44:1325–9.
- Kaasinen V, Ruottinen HM, Någren K, Lehtikoinen P, Oikonen V, Rinne JO. Upregulation of putaminal dopamine D2 receptors in early Parkinson's disease: a comparative PET study with [^{11}C]raclopride and [^{11}C]N-methylspiperone. *J Nucl Med* 2000;41:65–70.
- Rinne JO, Laihinen A, Rinne UK, Någren K, Bergman J, Ruotsalainen U. PET study on striatal dopamine D2 receptor changes during the progression of early Parkinson's disease. *Mov Disord* 1993;8:134–8.
- Dentresangle C, Veyre L, Le Bars D, Pierre C, Lavenne F, Pollak P, et al. Striatal D2 dopamine receptor status in Parkinson's disease: an [^{18}F]dopa and [^{11}C]raclopride PET study. *Mov Disord* 1999;14:1025–30.
- Antonini A, Schwarz J, Oertel WH, Pogarell O, Leenders KL. Long-term changes of striatal dopamine D2 receptors in patients

- with Parkinson's disease: a study with positron emission tomography and [^{11}C]raclopride. *Mov Disord* 1997;12:33–8.
22. Wang J, Zuo CT, Jiang YP, Guan YH, Chen ZP, Xiang JD, et al. 18F-FP-CIT PET imaging and SPM analysis of dopamine transporters in Parkinson's disease in various Hoehn & Yahr stages. *J Neurol* 2007;254:185–90.
 23. Knudsen GM, Karlsborg M, Thomsen G, Krabbe K, Regeur L, Nygaard T, et al. Imaging of dopamine transporters and D2 receptors in patients with Parkinson's disease and multiple system atrophy. *Eur J Nucl Med Mol Imaging* 2004;31:1631–8.
 24. Kim YJ, Ichise M, Ballinger JR, Vines D, Erami SS, Tatschida T, et al. Combination of dopamine transporter and D2 receptor SPECT in the diagnostic evaluation of PD, MSA, and PSP. *Mov Disord* 2002;17:303–12.
 25. Verstappen CC, Bloem BR, Haaxma CA, Oyen WJ, Horstink MW. Diagnostic value of asymmetric striatal D2 receptor upregulation in Parkinson's disease: an [^{123}I]IBZM and [^{123}I]FP-CIT SPECT study. *Eur J Nucl Med Mol Imaging* 2007;34:502–7.
 26. Fujiwara T, Watanuki S, Yamamoto S, Miyake M, Seo S, Itoh M, et al. Performance evaluation of a large axial field-of-view PET scanner: SET-2400W. *Ann Nucl Med* 1997;11:307–13.
 27. Hashimoto M, Kawasaki K, Suzuki M, Mitani K, Murayama S, Mishina M, et al. Presynaptic and postsynaptic nigrostriatal dopaminergic functions in multiple system atrophy. *Neuroreport* 2008;19:145–50.
 28. Ishibashi K, Ishii K, Oda K, Kawasaki K, Mizusawa H, Ishiwata K. Regional analysis of age-related decline in dopamine transporters and dopamine D2-like receptors in human striatum. *Synapse* 2009;63:282–90.
 29. NK LO, Dolle F, Lundkvist C, Sandell J, Swahn CG, Vaufrey F, et al. Precursor synthesis and radiolabelling of the dopamine D2 receptor ligand [^{11}C]raclopride from [^{11}C]methyl triflate. *J Labelled Compd Radiopharm* 1999;42:1183–93.
 30. Kawamura K, Oda K, Ishiwata K. Age-related changes of the [^{11}C]CFT binding to the striatal dopamine transporters in the Fischer 344 rats: a PET study. *Ann Nucl Med* 2003;17:249–53.
 31. Antonini A, Leenders KL, Reist H, Thomann R, Beer HF, Locher J. Effect of age on D2 dopamine receptors in normal human brain measured by positron emission tomography and ^{11}C -raclopride. *Arch Neurol* 1993;50:474–80.
 32. Nakajima K, Taki J, Tonami N, Hisada K. Decreased 123I-MIBG uptake and increased clearance in various cardiac diseases. *Nucl Med Commun* 1994;15:317–23.
 33. Gilman S, Low PA, Quinn N, Albanese A, Ben-Shlomo Y, Fowler CJ, et al. Consensus statement on the diagnosis of multiple system atrophy. *J Auton Nerv Syst* 1998;74:189–92.
 34. Litvan I, Agid Y, Calne D, Campbell G, Dubois B, Duvoisin RC, et al. Clinical research criteria for the diagnosis of progressive supranuclear palsy (Steele-Richardson-Olszewski syndrome): report of the NINDS-SPSP international workshop. *Neurology* 1996;47:1–9.
 35. Li ST, Dendi R, Holmes C, Goldstein DS. Progressive loss of cardiac sympathetic innervation in Parkinson's disease. *Ann Neurol* 2002;52:220–3.
 36. Braune S. The role of cardiac metaiodobenzylguanidine uptake in the differential diagnosis of parkinsonian syndromes. *Clin Auton Res* 2001;11:351–5.
 37. Spiegel J, Mollers MO, Jost WH, Fuss G, Samnick S, Dillmann U, et al. FP-CIT and MIBG scintigraphy in early Parkinson's disease. *Mov Disord* 2005;20:552–61.
 38. Fearnley JM, Lees AJ. Ageing and Parkinson's disease: substantia nigra regional selectivity. *Brain* 1991;114(Pt 5):2283–301.
 39. Guttman M, Seeman P, Reynolds GP, Riederer P, Jellinger K, Tourtellotte WW. Dopamine D2 receptor density remains constant in treated Parkinson's disease. *Ann Neurol* 1986;19:487–92.
 40. Bokobza B, Ruberg M, Scatton B, Javoy-Agid F, Agid Y. [^3H] spiperone binding, dopamine and HVA concentrations in Parkinson's disease and supranuclear palsy. *Eur J Pharmacol* 1984;99:167–75.
 41. Kish SJ, Shannak K, Hornykiewicz O. Uneven pattern of dopamine loss in the striatum of patients with idiopathic Parkinson's disease. Pathophysiologic and clinical implications. *N Engl J Med* 1988;318:876–80.

Expanding the Clinical Phenotype of SNCA Duplication Carriers

Kenya Nishioka, MD, PhD,^{1,2} Owen A. Ross, PhD,² Kenji Ishii, MD,³ Jennifer M. Kachergus, BS,² Kiichi Ishiwata, PhD,³ Mayumi Kitagawa, MD, PhD,⁴ Satoshi Kono, MD, PhD,⁵ Tomokazu Obi, MD, PhD,⁶ Koichi Mizoguchi, MD, PhD,⁶ Yuichi Inoue, MD, PhD,⁷ Hisamasa Imai, MD, PhD,⁸ Masashi Takanashi, MD, PhD,¹ Yoshikuni Mizuno, MD,¹ Matthew J. Farrer, PhD,² and Nobutaka Hattori, MD, PhD^{1*}

¹Department of Neurology, Juntendo University School of Medicine, Bunkyo-ku, Tokyo, Japan

²Division of Neurogenetics, Department of Neuroscience, Mayo Clinic, Jacksonville, Florida, USA

³Tokyo Metropolitan Institute of Gerontology, Itabashi-ku, Tokyo, Japan

⁴Department of Neurology, Sapporo Azabu Neurosurgical Hospital, Higashi-ku, Sapporo, Japan

⁵Department of Neurology, Hamamatsu University School of Medicine, Shizuoka, Japan

⁶Department of Neurology, Shizuoka Institute of Epilepsy and Neurological Disorders, Shizuoka, Japan

⁷Japan Somnology Center, Neuropsychiatric Research Institute, Shibuya-ku, Tokyo, Japan

⁸Department of Neurology, Tokyo Rinkai Hospital, Edogawa-ku, Tokyo, Japan

Abstract: SNCA duplication is a recognized cause of familial Parkinson's disease (PD). We aimed to explore the genetic and clinical variability in the disease manifestation. Molecular characterization was performed using real-time PCR, SNP arrays, and haplotype analysis. We further studied those patients who were found to harbor SNCA duplication with olfactory function tests, polysomnography, and PET. We identified four new families and one sporadic patient with SNCA duplication. Eleven symptomatic patients from these four families presented with parkinsonism, of which three subsequently developed dementia. The lifetime estimate of overall penetrance was 43.8%. FDG–PET study of symptomatic patients showed hypometabolism in the occipital lobe, whereas asymptomatic carriers of SNCA duplication demon-

strated normal glucose metabolism. Symptomatic patients showed abnormal olfactory function and polysomnography and asymptomatic carriers showed normal results. The clinical features of SNCA duplication include parkinsonism with or without dementia. Asymptomatic carriers displayed normal test results with the eldest individual aged 79 years; thus, even a carrier of SNCA duplication may escape the development of PD. This difference in age-associated penetrance may be due to the genetic background or environmental exposures. Further studies of SNCA duplication carriers will help identify disease-modifiers and may open novel avenues for future treatment. © 2009 Movement Disorder Society

Key words: Parkinson's disease; SNCA duplication; PET; dementia; reduced penetrance

The cardinal features of Parkinson's disease (PD) include rest tremor, rigidity, bradykinesia, and postural instability. The pathologic hallmark is neuronal degeneration in the substantia nigra and locus coeruleus with

Lewy bodies in the surviving neurons.¹ The reason for selective vulnerability and neuronal loss in sporadic PD is not known yet.

Mutations of the SNCA gene have been observed to result in familial PD with similar clinical and pathologic features to those present in the sporadic form of the disease. In addition to three coding substitutions in the α -synuclein protein (p.A30P, p.E46K, and p.A53T), genomic multiplication of chromosome 4q21-22, containing the SNCA locus has also been linked to autosomal dominant PD with or without dementia.^{2–13} In contrast with the parkinsonism and dementia associated with SNCA triplication, clinical features of monoallelic duplication (three copies of SNCA) are

Additional Supporting Information may be found in the online version of this article.

*Correspondence to: Dr. Nobutaka Hattori, Department of Neurology, Juntendo University School of Medicine, 2-1-1 Hongo, Bunkyo-ku, Tokyo 113-8421, Japan. E-mail: nhattori@juntendo.ac.jp

Potential conflict of interest: The authors declare no financial or other conflicts of interest.

Received 28 January 2009; Revised 25 March 2009; Accepted 27 May 2009

Published online 26 June 2009 in Wiley InterScience (www.interscience.wiley.com). DOI: 10.1002/mds.22682

essentially those of sporadic PD without dementia, although generally with an earlier age at onset.^{12,13} Recently, we reported a Japanese patient with parkinsonism and dementia resulting from *SNCA* duplication, who was pathologically diagnosed as diffuse Lewy body disease (DLBD).¹⁴ These pathologic findings are reminiscent of those observed in some *SNCA* triplication patients.^{15,16}

Herein, we report our screening of *SNCA* multiplication in both familial and sporadic PD patients, in which we found four new families and one apparently sporadic patient with *SNCA* duplication. Furthermore, within our families, we observed 14 asymptomatic carriers with *SNCA* duplication. We studied our patients and asymptomatic carriers with olfactory tests, brain MRI, PET using [¹¹C]-RAC, [¹¹C]-CFT, and [¹⁸F]-FDG, and polysomnography (PSG). We report motor and non-motor features as well as laboratory aspects of *SNCA* duplication in symptomatic and asymptomatic subjects.

SUBJECTS AND METHODS

Subjects of Gene Dosage Analysis

We studied 103 consecutive patients with autosomal dominant PD [43 male and 60 female with a mean age at onset of 50.9 ± 13.9 years (\pm SD)] who had at least one affected individual within one degree of separation, and 71 patients (29 male and 42 female with 37.7 ± 13.0 years) with sporadic PD. We reported Family A and B previously.¹¹ Diagnosis of PD was made according to the United Kingdom Parkinson's Disease Society Brain Bank criteria by participating neurologists (KN, YM, and NH).¹⁷ All the patients studied were Japanese and a summary of the clinical data is presented in Table 1. The study was approved by the ethics review committee of Juntendo University. We obtained written informed consent from all the patients in whom blood samples were collected for genetic analyses.

Gene Dosage and Haplotype Analysis on *SNCA* Locus

DNA was prepared according to standard methods from peripheral blood.¹⁸ Mutation screening was performed as previously described.¹¹ *SNCA* duplication was confirmed with copy number variation analysis using the Affymetrix 250K SNP array (Affymetrix, Santa Clara, CA) as described previously.⁷ DNA samples for all available family members were genotyped for short tandem repeat markers flanking the *SNCA* locus (D4S3475, D4S3477, D4S3480, D4S3479, and

D4S3474) using fluorescent-labeled primers, ABI PRISM 3730 DNA Analyzer, and Genemapper software version 4.0 (Applied Biosystems, CA). All PCR conditions, primer and probe sequences are available upon request.

PET Studies

Four symptomatic familial patients (A-II-9, A-II-11, C-III-3, and E-III-6), and three asymptomatic carriers (A-II-2, A-II-4, and A-III-3) were studied by [¹¹C]-labeled 2 β -carbomethoxy-3 β -(4-fluorophenyl)-tropane (CFT) and [¹¹C]-labeled raclopride (RAC). Demographics of each group are shown in Table 2. We also examined comparison groups of sporadic PD patients with Hoehn and Yahr stage I (n = 10, male (m):female (f) = 5:5; mean age at exam 58.6 ± 9.57 years), stage II (n = 18, m:f = 9:9; CFT 66.6 ± 9.87 years; RAC 65.3 ± 9.22 years), and stage III disease (n = 9, m:f = 2:7; CFT 66.5 ± 10.3 years; RAC 65.8 ± 10.6 years), and normal controls (n = 7, m:f = 4:3; CFT; 59.4 ± 5.00 years; RAC; 60.9 ± 5.59 years). The same symptomatic familial patients and asymptomatic carriers, and an additional normal control group (n = 30, m:f = 12:18; 52.9 ± 3.9 years) were analyzed for [¹⁸F]-labeled 2-fluoro-2-deoxy-D-glucose (FDG).

PET studies were performed in the Positron Medical Center, Tokyo Metropolitan Institute of Gerontology Positron Medical Center with a HEADTOME V scanner (Shimazu, Kyoto, Japan).¹⁹ All anti-Parkinson drugs were discontinued for at least 12 hours before dopaminergic scanning. We used [¹¹C]-CFT for dopamine transporter imaging and [¹¹C]-RAC for dopamine receptor imaging; these imaging studies were performed on the same day. Cerebral glucose metabolism was evaluated with FDG on a different day within a week from the dopaminergic PET study.

PET image manipulations were carried out using the medical image processing application package "Dr View/LINUX" version R2.0 (AJS, Tokyo, Japan) and SPM2 (The Wellcome Department of Imaging Neuroscience, Institute of Neurology, University College London, London, UK) implemented in MATLAB version 7.0.1 (MathWorks, Natick, MA). Regions of interest were placed on PET images with reference to individual co-registered MRI on the cerebral hemisphere, caudate nucleus, and striatum on each side. The activity was calculated using the ratio index (i.e., target region of interest activity—cerebellar activity/cerebellar activity) that is linearly correlated with the regional binding potential of [¹¹C]-CFT. For visual inspection, a

TABLE 1. Clinical data of SNCA duplication patients

Heredity	Autosomal dominant										Sporadic	
	A-II-9 (+)	A-II-11 (+)	B-II-7 (+)	C-III-3 (+)	D-III-1 (+)	D-III-5 (+)	E-III-4 (+)	E-III-6 (+)	F-II-5 (+)	F-III-2 (+)		G-III-1 (+)
SNCA duplication												
Gender/age at last exam	F/58	M/44	M/67	F/57	F/57	M/46	F/66	M/57	M/68	M/40	M/35	
Age at onset	48	38	47	49	56	38	54	53	62	37	31	
Symptom at onset	Gait disturbance	Gait disturbance	Rigidity on the left hand	Bradykinesia on right hand	Bradykinesia on right hand	Bradykinesia on left hand	Bradykinesia	Bradykinesia on right hand	Rigidity on right hand	Tremor on left hand	Bradykinesia on right hand	
DD	10	7	21	9	2	9	13	5	7	4	5	
UPDRS (on)	28/199	37/199	Bed ridden	20/199	17/199	31/199	95/199	23/199	58/199	17/199	13/199	
Hoehn and Yahr stage (on)	III	III	V	III	II	II	V	II	III	II	II	
MMSE	28/30	26/30	0/30	27/30	30/30	30/30	7/30	28/30	19/30	30/30	28/30	
HDSR	29/30	24/30	0/30	27/30	30/30	29/30	8/30	28/30	19/30	29/30	30/30	
Beck	32	20	(-)	5	0	1	(-)	4	10	15	24	
Hamilton	14	9	(-)	6	0	1	(-)	0	15	12	29	
Hallucination or delusion	(+)	(-)	(++)	(-)	(-)	(-)	(+++)	(-)	(++)	(+)	(+)	
Olfactory dysfunction	(+)	(+)	NK	(+)	NK	NK	NK	(+)	NK	(+)	(+)	
RBD	(+)	(+)	NK	(-)	(-)	(-)	NK	(-)	NK	(-)	(+)	
Response to levodopa	Moderate	Moderate	Early good, Later no effect	Moderate	Good	Good	Early good, Later no effect	Good	Poor	Good	Good	

Clinical symptoms of 11 patients were assessed. Rigidity and akinesia are the main symptoms, and tremor was less problematic. Dementia and severe cognitive decline was observed in three patients (B-II-7, E-III-4, and F-II-5). Hallucination was also a marked symptom (6/11).
M, male; F, female; NK, not known; DD, disease duration; UPDRS, unified Parkinson's disease rating scale; H and Y stage, Hoehn and Yahr stage; MMSE, mini-mental state examination; HDS-R, revised Hasegawa dementia scale; RBD, REM sleep behavior disorder.

TABLE 2. Comparison of [¹¹C]-labeled 2β-carbomethoxy-3β-(4-fluorophenyl)-tropine

No. samples	Age ± SD	Gender (m:f)	Caudate mean ± SD	P-value			P-value			P-value					
				SNCA dup	HYIII	AC	SNCA dup	HYIII	AC	SNCA dup	HYIII	AC			
SNCA dup	4	52.8 ± 5.63	2:2	2.13 ± 0.45	1.52 ± 0.20	1.35 ± 0.11	0.001	0.001	0.001	0.001	0.001	0.001	0.001	0.001	0.001
PD HYIII	10	66.5 ± 10.3	3:7	3.18 ± 0.31	2.72 ± 0.45	2.10 ± 0.30	0.03	0.004	0.03	0.004	0.004	0.03	0.004	0.004	0.004
AC	3	53.3 ± 16.0	1:2	3.81 ± 0.27	3.98 ± 0.26	3.65 ± 0.26	0.003	0.007	0.03	0.003	0.004	0.003	0.003	0.004	0.004
NC	7	59.4 ± 5.00	4:3	4.29 ± 0.56	4.44 ± 0.58	4.02 ± 0.40	0.003	<0.0001	0.09	<0.0001	0.09	0.003	<0.0001	<0.0001	0.06

Displays the comparative statistics examining differences in [¹¹C]CFT between four sample groups.

Significantly different P-values were highlighted in bold (significance threshold was assessed at the $P > 0.05$ level).

PD H and Y III, sporadic Parkinson's disease patients with Hoehn and Yahr stage III disease; SNCA dup, patients with SNCA duplication; AC, asymptomatic carriers; NC, normal controls.

mapping image of the ratio index was created. Statistical analysis was performed using the Mann-Whitney test.

All FDG-PET images were spatially normalized to a standard template produced by Montreal Neurological Institute using an in-house template of FDG-PET images and smoothed with Gaussian filter for 16 mm FWHM to increase the signal-to-noise ratio before statistical processing. A group effect of affected subjects ($n = 4$) and unaffected subjects ($n = 3$) was estimated in comparison with healthy control subjects using ANCOVA (analysis of covariance) statistics excluding the aging effect. We selected global normalization proportional scaling in global normalization. Statistical inference on the SPM (statistical parametric mapping) was corrected using the theory of Gaussian Fields. The threshold for SPM was set at $P < 0.05$, corrected for multiple comparisons.

Evaluation of REM Sleep Behavior Disorder

We assessed REM (rapid eye movement) sleep behavior disorder (RBD) in six affected patients (A-II-9, A-II-11, C-III-3, E-III-6, F-III-2, and G-III-1; 47.8 ± 9.21 years; m:f = 4:2) and three asymptomatic carriers (A-II-2, A-II-4, and A-III-3; 53.3 ± 16.0 years; m:f = 1:2) according to the criteria on the International Classification of Sleep Disorder (ICSD), second edition²⁰; and PSG was performed using the standard package of Alice 4 (Respironics, Pittsburgh, PA). The analysis of PSG data was performed using the standard criteria of Rechtschaffen and Kales and the EEG arousals were scored using the American Sleep Disorders Academy Guidelines.^{20,21} The diagnostic criteria for REM without atonia were previously described.²²

Olfactory Testing

We studied olfactory threshold (OT), odor discrimination (OD), and odor identification (OI) in three separate subtests using standardized "Sniffin" Sticks' (Burghardt, Wedel, Germany). These protocols were previously described in detail.^{23,24} Six patients (with 47.8 ± 9.22 years; m:f = 4:2) A-II-9, A-II-11, C-III-3, E-III-6, F-III-2, and G-III-1, five asymptomatic carriers (64.6 ± 16.0 years; m:f = 1:4) A-II-2, A-II-4, A-III-3, G-II-4, and G-II-5, and 22 normal controls (64.9 ± 10.1 years; m:f = 10:12). Normative values according to Hummel et al. for 51 to 80 years control: OT; male, 7.1 ± 1.7 ; female, 7.7 ± 2.6 ; OD; male, 10.6 ± 1.8 ; female, 10.6 ± 1.0 ; OI; male, 14.2 ± 1.5 ; female, 13.3 ± 1.5 .²⁵ Statistical significance was set at $P < 0.05$ by

means of Student *t*-test. Results are reported as mean \pm standard deviation.

RESULTS

Summary of Clinical Features

All the pedigrees studied are shown in Figure 1 and clinical data of 11 patients (m:f = 8:3; 48.5 ± 11.1 years) are presented in Table 1 (detailed clinical information is provided as supplementary data). All 11 patients harbored *SNCA* duplication and presented with parkinsonism consisting mostly of rigidity and bradykinesia, tremor being less prominent. Two patients had slight tremor, five patients had no tremor. Three patients (B-II-7, E-III-4, and F-III-2) had dementia with MMSE (mini-mental state examination) scores under 20. The clinical features of these three patients were consistent with a clinical diagnosis of PD with dementia (PDD); patients with a disease duration <10 years had milder parkinsonism. Parkinsonism was the initial symptom in all ($n = 11$). Two patients (B-II-7 and E-III-4) had severe disease with a Hoehn and Yahr stage V. In the subsequent clinical course, six patients developed hallucinations and/or delusions and three patients (A-II-9, A-II-11, and F-III-2) had severe depression. Disease penetrance among carriers was age-associated and a lifetime estimate of overall penetrance in seven families was 43.8%.

Genomic Analysis of *SNCA* Duplication

Haplotypes were constructed using five microsatellite markers in the *SNCA* region (Fig. 1). Analysis indicates three possible independent allele sharing for (1) Family A and F, (2) Family B and C, and (3) Family D and G. No allele sharing was observed for Family E suggesting a *de novo* event (Fig. 1). Real time PCR analysis showed that two pedigrees (Family A and F) had a duplication of the *SNCA* locus and only a part of the *MMRN1* gene (supplementary Fig. 1); whereas the other families studied had a duplication of the *SNCA* locus and the entire *MMRN1* gene. The Affymetrix SNP 250K array confirmed the results of quantitative PCR. Family E had the smallest duplicated region (0.2Mb) including the *SNCA* locus (Fig. 2). All patients were negative for *PARKIN*, *PINK1*, or *DJ-1* mutations.

PET Studies

Our four patients with a *SNCA* duplication showed severe reductions of dopamine transporters in the ante-

rior and posterior putamen and caudate by [^{11}C]-CFT PET. *P*-values were < 0.05 between asymptomatic carriers, PD with Hoehn and Yahr stage III, and normal controls subjects (Table 2 and Fig. 3A). [^{11}C]-CFT PET showed a more severe reduction of dopamine transporters in patients with *SNCA* duplication compared to sporadic PD patients, although both groups had the same Hoehn and Yahr stage III: caudate ($P = 0.001$), anterior putamen ($P = 0.001$), and posterior putamen ($P = 0.001$).

On [^{11}C]-RAC PET, dopamine D_2 receptor density was overall similar to normal controls. However, interestingly, we observed a severe reduction in D_2 receptor density in the caudate of patients with *SNCA* duplication [2.84 ± 0.15 (\pm SD)] compared to asymptomatic carriers (4.09 ± 0.25 ; $P = 0.029$), PD patients with Hoehn and Yahr stage III disease (4.45 ± 0.53 ; $P = 0.001$), and normal control subjects (4.46 ± 0.38 ; $P = 0.003$). Regarding the FDG-PET study, our results showed significantly reduced glucose metabolism in the parieto-temporo-occipital cortex bilaterally (Fig. 3B), the three asymptomatic carriers showed normal findings (data not shown).

REM Sleep Behavior Disorder

Only patient A-II-9 had RBD out of six patients with *SNCA* duplication examined. She experienced oneiric behavior while dreaming, and had REM sleep without atonia (RWA) on PSG, an important finding in the diagnosis of RBD.²⁶ Patient A-II-11 reported an experience of shouting, standing up and kicking in bed for a few minutes while sleeping. He was diagnosed as possible RBD because definite RWA was not observed on PSG. All three asymptomatic carriers did not report any abnormal behaviors during sleep and their PSGs were normal.

Olfactory Testing

The values for patients with *SNCA* duplication were OT; 2.25 ± 1.63 , OD; 6.67 ± 2.58 , and OI; 5.83 ± 3.19 , for asymptomatic carriers OT; 6.9 ± 3.27 , OD; 11.6 ± 1.82 , and OI; 10.0 ± 4.95 , and for normal controls OT; 7.67 ± 1.76 , OD; 11.1 ± 2.33 , and OI; 10.6 ± 1.79 . The patients with *SNCA* duplication showed severe reduction in OT, OD, and OI compared to normal controls ($P < 0.0005$), and in OT and OD compared to asymptomatic carriers ($P < 0.05$). There were no differences between asymptomatic carriers and normal controls ($P > 0.05$; Fig. 3C).

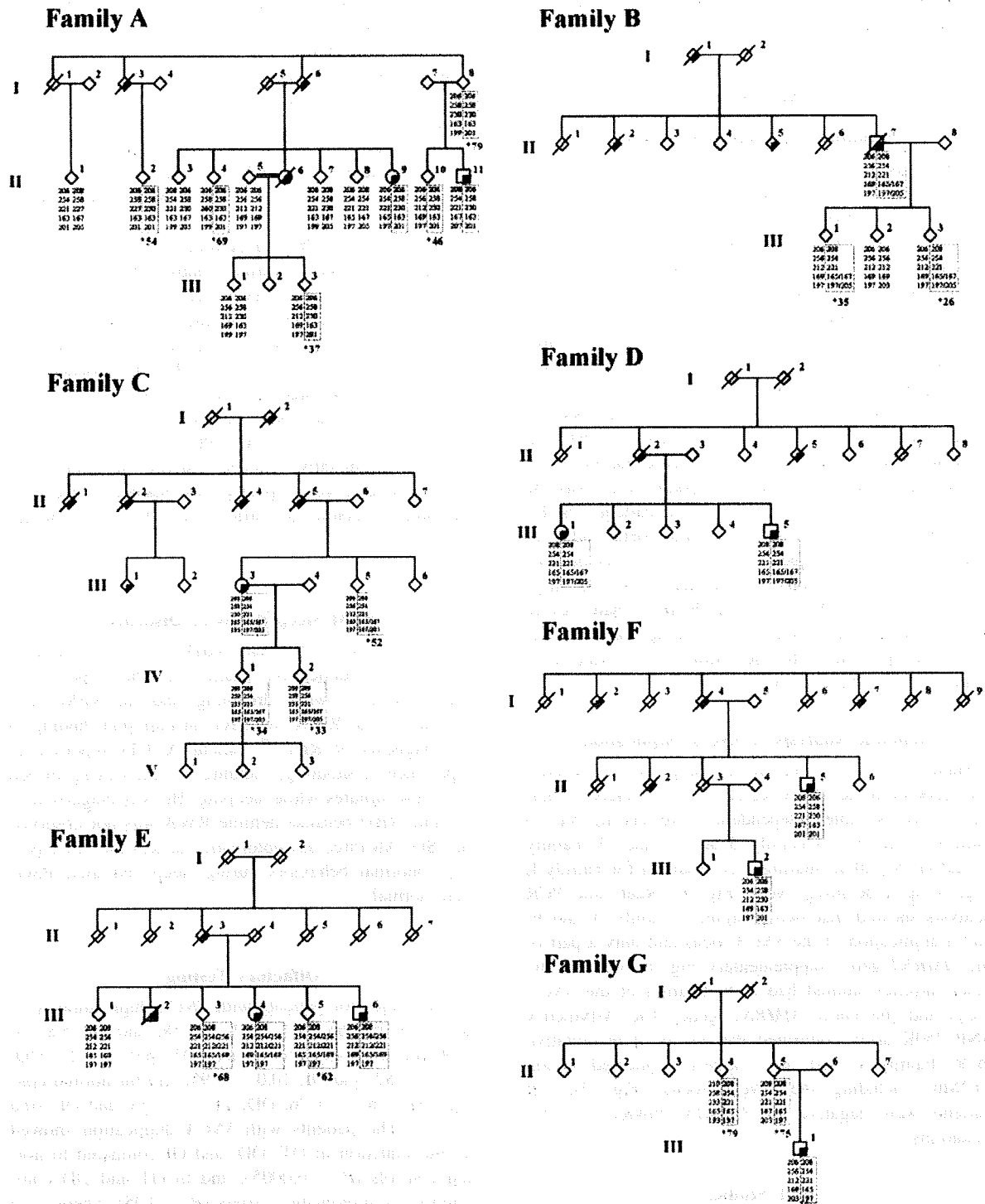


FIG. 1. Pedigrees of *SNCA* duplication families and haplotype analysis. The pedigrees with *SNCA* duplication are shown. Affected patients with parkinsonism are represented with a quarter-filled symbol and asymptomatic carriers with an asterisk with each age under genotyping results. Box with dot line around allele indicates duplicated allele. Families A and F (prefecture Nagano) and Families B, C, and D (prefecture Shizuoka) come from the same rural area of Japan. A-II-4, A-I-8, and G-II-5 were asymptomatic carriers older than 70 years of age. Haplotype markers (D4S3475, D4S3477, D4S3480, D4S3479, and D4S3474) in the *SNCA* region showed the possible existence of four founders in the seven duplication pedigrees of Japanese origin.

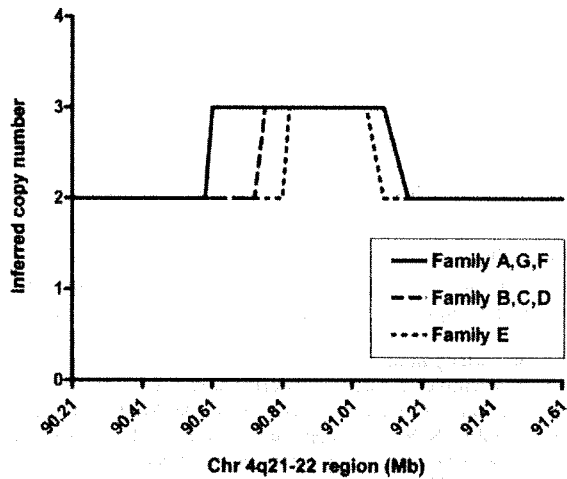


FIG. 2. Analysis of gene chip mapping 250K array. The assessment of copy number variation based on analysis of GeneChip Mapping 250K. Array data for chromosome 4q21, 90.21- to 91.61- Mb centromeric to telomeric. A value of 2.0 indicates normal diploid copy number. These results demonstrate three different regions and three copy numbers (monoallelic duplication). Patients A-II-9 and B-II-7 have been previously confirmed by this method and herein, C-III-3, D-III-5, E-III-6, F-III-2, and G-III-1 were examined.¹²

DISCUSSION

Herein, we describe four new *SNCA* duplication pedigrees and one apparent sporadic PD patient. In total, our *SNCA* duplication patients of Japanese ethnicity came from six pedigrees and one sporadic case. In addition, haplotype analysis of the seven families indicates four independent founder events (Fig. 1). All the duplicated regions in our families share the entire *SNCA* gene (Fig. 2), thus we hypothesize that multiple copies of *SNCA* alone can cause parkinsonism with or without dementia.

The average age of onset in *SNCA* duplication patients is 15 years older than that of *SNCA* triplication individuals suggesting that the copy number variation influences the clinical severity and the rate of progression.²⁷ Our study demonstrates that the clinical features of *SNCA* duplication vary even within the same family as seen in Family B, E, and F. Three patients developed dementia, whereas 14 persons did not show symptoms despite harboring a duplication of *SNCA*; age of onset ranged from 31 to 69 years (average 48.5 ± 11.2) in these families. Eight of the 11 patients

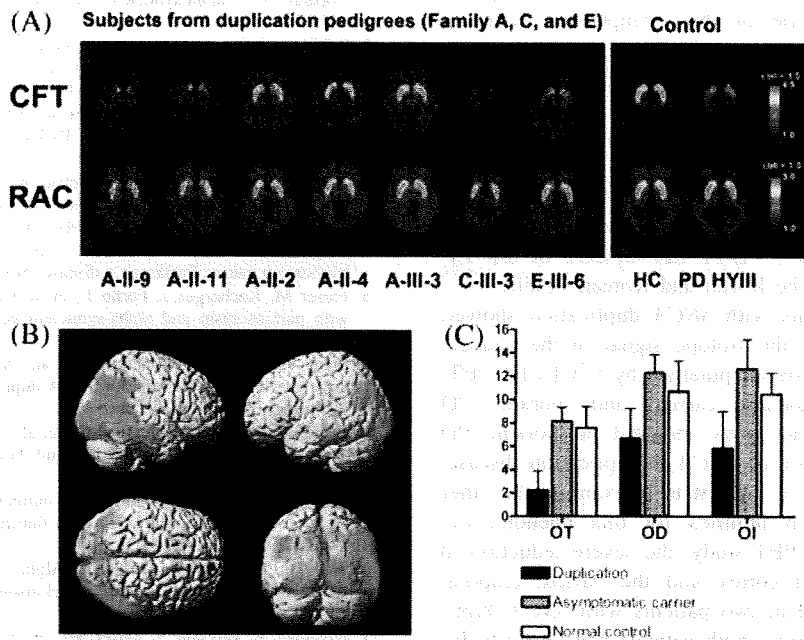


FIG. 3. PET study and olfactory testing. (A) The PET study of duplication patients was performed with CFT and RAC. A severe reduction of dopamine transporters was demonstrated in bilateral caudate and putamen at CFT in all affected patients. Asymptomatic carriers did not show any reduction in CFT and RAC. (B) FDG-PET. SPM was performed allowing exploratory voxel by voxel group comparisons throughout the entire brain volume ($P < 0.05$, $k < 300$). Four patients with *SNCA* duplication and 30 normal controls were evaluated. Significant reductions of FDG signal were localized in the occipital lobe of *SNCA* duplication patients (composite image of all four patients shown). (C) Olfaction was assessed by "Sniffin" sticks' (Burghardt, Wedel, Germany) for Olfactory Threshold (OT), odor Discrimination (OD), and odor Identification (OI). Five patients, five asymptomatic carriers (AC), and 22 normal controls (NC) were assessed. Reduced levels were seen in the patients with *SNCA* duplication in all OT, OD, and OI, as opposed to NC and AC.

(72.7%) had a good response to levodopa and a milder course without developing dementia. In addition, six of our 11 (54.5%) *SNCA* duplication patients had visual hallucinations including five in whom they occurred within 10 years of disease duration. PDD patients have a higher prevalence of hallucinations and delusions (45–65%) than PD patients (25%).^{28,29} The prevalence of visual hallucination in our patients with *SNCA* duplication was similar to that of PDD patients. Interestingly, progressive myoclonus epilepsy type 1 (EPM1) is reported in the Lister family (17/1909 compared to the Swedish EPM prevalence of 1;20,000), however, only one of our patients (B-III-3) had a history of frontal lobe epilepsy without myoclonus.³⁰

Remarkably three asymptomatic carriers were over 70 years of age without any signs of parkinsonism or dementia (Fig. 1 and supplementary Fig. 2). The calculated lifetime penetrance ratio was 43.8%. The same penetrance values (33–50%) have also been observed in Korean *SNCA* duplication pedigrees.¹⁰ Before this study, we thought that asymptomatic carriers may already have pre-motor olfactory problems or sleep disorders, based on the Braak hypothesis; olfactory dysfunction or RBD are reported in early stage of PD.³¹ However, none of the asymptomatic carriers studied demonstrated any motor or non-motor symptoms. These findings suggest that not only genetic factors but also environmental exposure, modifier genes, or aging influence the development of the disease in *SNCA* duplication individuals.

PET and SPECT studies in *SNCA* multiplication families have previously demonstrated severe reduction in striate uptake by [¹²³I]-FP-CIT SPECT or 6-[¹⁸F]-fluorodopa PET in the Iowan and Korean families.^{10,15} Of note, our patients with *SNCA* duplication showed severe reduction of the isotope signal in the caudate and anterior and posterior putamen by [¹¹C]-CFT PET, unlike our asymptomatic carriers and sporadic PD patients. This has not been observed in sporadic PD and may be a feature of *SNCA* multiplication disease, therefore it will be of interest to re-examine the other *SNCA* multiplication families for this phenomenon. According to FDG-PET study, the severe reduction in posterior cingulate cortex and the parieto-temporal cortex was reported in two patients with *SNCA* duplication from one family; both patients had visual hallucination. Their findings are similar to those of our four patients with *SNCA* duplication. Hypoperfusion or hypometabolism in the occipital association cortex on FDG-PET is frequently observed in patients with DLB.^{32–34} In conclusion, PET studies on *SNCA* duplication patients show similarities with DLB, whereas

that of asymptomatic carriers did not show any change.

Our study indicates that motor and non-motor symptoms in patients with *SNCA* duplication are heterogeneous. Asymptomatic carriers did not have any abnormalities both clinically and in examination of PET, olfactory test, and PSG, even at >70 years of age. These results suggest that in addition to copy number variation, other factors influence the development of symptoms in subjects with *SNCA* duplications.

Acknowledgments: This work was supported by grant-in-aid for scientific research on priority areas (research on pathomechanisms of brain disorders) from the MEXT of Japan (#20023028). K.N. was supported by a Eli-Lilly scholarship and a Herb Geist gift for Lewy body research. We would like to thank Hiroyo Yoshino and Yoko Imamichi (Juntendo University) for management of all DNA samples, Kazuyoshi Namba (Yoyogi sleep disorder clinic) for analyzing PSG, and Haruo Hanyu (Tokyo Medical University) for providing clinical information of Patient E-III-2.

REFERENCES

1. Spillantini MG, Schmidt ML, Lee VM, Trojanowski JQ, Jakes R, Goedert M. Alpha-synuclein in Lewy bodies. *Nature* 1997; 388:839–840.
2. Polymeropoulos MH, Lavedan C, Leroy E, et al. Mutation in the alpha-synuclein gene identified in families with Parkinson's disease. *Science* 1997;276:2045–2047.
3. Kruger R, Kuhn W, Muller T, et al. Ala30Pro mutation in the gene encoding alpha-synuclein in Parkinson's disease. *Nat Genet* 1998;18:106–108.
4. Zarranz JJ, Alegre J, Gomez-Esteban JC, et al. The new mutation, E46K, of alpha-synuclein causes Parkinson and Lewy body dementia. *Ann Neurol* 2004;55:164–173.
5. Singleton AB, Farrer M, Johnson J, et al. Alpha-synuclein locus triplication causes Parkinson's disease. *Science* 2003;302:841.
6. Farrer M, Kachergus J, Forno L, et al. Comparison of kindreds with parkinsonism and alpha-synuclein genomic multiplications. *Ann Neurol* 2004;55:174–179.
7. Fuchs J, Nilsson C, Kachergus J, et al. Phenotypic variation in a large Swedish pedigree due to *SNCA* duplication and triplication. *Neurology* 2007;68:916–922.
8. Ibanez P, Bonnet AM, Debarges B, et al. Causal relation between alpha-synuclein gene duplication and familial Parkinson's disease. *Lancet* 2004;364:1169–1171.
9. Chartier-Harlin MC, Kachergus J, Roumier C, et al. Alpha-synuclein locus duplication as a cause of familial Parkinson's disease. *Lancet* 2004;364:1167–1169.
10. Ahn TB, Kim SY, Kim JY, et al. Alpha-synuclein gene duplication is present in sporadic Parkinson disease. *Neurology* 2008;70:43–49.
11. Nishioka K, Hayashi S, Farrer MJ, et al. Clinical heterogeneity of alpha-synuclein gene duplication in Parkinson's disease. *Ann Neurol* 2006;59:298–309.
12. Ross OA, Braithwaite AT, Skipper LM, et al. Genomic investigation of alpha-synuclein multiplication and parkinsonism. *Ann Neurol* 2008;63:743–750.
13. Ikeuchi T, Kakita A, Shiga A, et al. Patients homozygous and heterozygous for *SNCA* duplication in a family with parkinsonism and dementia. *Arch neurol* 2008;65:514–519.